Available online at www.sciencedirect.com
SCIENCE DIRECT
Polymer 46 (2005) 2105–2121
polymer
www.elsevier.com/locate/polymer

# Liquid crystalline elastomers based on diglycidyl terminated rigid monomers and aliphatic acids. Part 1. Synthesis and characterization

Veronica Ambrogi[a,*], Marta Giamberini[b], Pierfrancesco Cerruti[a], Piero Pucci[d], Nicola Menna[a], Rita Mascolo[a], Cosimo Carfagna[a,d]

[a]*Dipartimento di Ingegneria dei Materiali e della Produzione, Università di Napoli 'Federico II', Piazzale Tecchio 80, 80125 Napoli, Italy*
[b]*Istituto per i Materiali Compositi e Biomedici, IMCB-Consiglio Nazionale delle Ricerche, Piazzale Tecchio 80, 80125 Napoli, Italy*
[c]*Dipartimento di Chimica Organica e Biochimica, ICTP-Consiglio Nazionale delle Ricerche, Via Campi Flegrei 34, 80078 Pozzuoli (Na), Italy*
[d]*Istituto di Chimica e Tecnologia dei Polimeri, Università di Napoli 'Federico II', Via Cinthia 6, 80126 Napoli, Italy*

Received 5 November 2004
Available online 28 January 2005

**Abstract**

Liquid crystalline elastomers (LCEs) were prepared by reacting rigid-rod mesogenic epoxy monomers with aliphatic diacids of variable length. The influence of acid and nature of epoxy monomer on the mechanism of network growth was investigated through DSC, FT-IR, MALDI, $^{1}H$ and $^{13}C$ NMR and rheological experiments. Depending on the nature of epoxy monomer, different mechanisms of network growth occurred, which were responsible for the formation of elastomers with different extent of branching.

Clearing temperatures, enthalpies and entropies, and the nature of mesophases were also analyzed through DSC and X-ray diffraction, carried out on unstrained elastomers. It was found that both the rigid-rod mesogens and the aliphatic portions of carboxylic acids contribute to stabilize the mesophase. Moreover, upon stretching, all the LCEs exhibited the polydomain-to-monodomain transition, which is typical of this class of materials.


*Keywords:* Liquid crystalline elastomers; Epoxy resins; Aliphatic acids

## 1. Introduction

Liquid crystalline elastomers (LCEs) are lightly crosslinked networks, in which rigid-rod, mesogenic moieties are incorporated into (main-chain LCEs) or linked to (side-chain LCEs) the polymer backbone [1–4]. A detailed classification of polymer liquid-crystals (PLCs) is reported in [5]. LCEs typically exhibit glass transition temperatures around room temperature and low elastic moduli. Moreover, due to the high mobility of the network segments, they exhibit reversible transition from the liquid crystalline to the isotropic phase on heating [4,6].

Over the past decades, LCEs have been extensively studied, since the simultaneous presence of rubber elasticity, due to the crosslinked backbone chains, and optical birefringence, related to the mesogens, lead to exceptional physical properties. An elastic deformation of the network influences the order of the mesogens and, therefore, the optical properties. In particular, they can undergo a stress-induced polydomain-to-monodomain transition. Moreover, they exhibit many remarkable features, such as spontaneous shape changes at LC phase transitions, and unique dynamic-mechanical properties [7–12].

Finkelmann et al. reported the synthesis and characterization of the side-chain liquid crystalline elastomers, which showed macroscopic optical properties similar to an anisotropic single crystal when oriented by mechanical stress [4,13]. They discussed the effect of mechanical deformation on the mesophase stability, and found an increase of the phase transformation temperature with stress as predicted by Landau-de Gennes theory [14–16]. Since then, a wide range of synthetic side-chain elastomers have been described in literature [17–21].

* Corresponding author. Tel.: +39 081 768 2510; fax: +39 081 768 2404.
*E-mail address:* ambrogi@unina.it (V. Ambrogi).

0032-3861/$ - see front matter © 2005 Elsevier Ltd. All rights reserved.
doi:10.1016/j.polymer.2005.01.007

On the other hand, fewer papers were published on the synthesis and characterization of main-chain LCEs [22–25].

The development of main-chain LCE was based on different chemical structures. Zentel prepared combined main/side-chain elastomers based on polyacrylates, polymethacrylates and polymalonates. These systems exhibited a wide variety of phases including $S_A$, $S_C$, $S_C$*, $S_B$, and nematic, as well as cholesteric [22].

Percec et al. synthesized main-chain liquid crystalline polyethers based on semiflexible mesogenic groups connected by flexible alkyl spacers [23].

More recently, a new LC elastomeric network was synthesized via a main-chain polyether, and characterized in terms of orientational behaviour and mechanical properties [24].

In their work, Rousseau and Mater have designed and prepared main-chain LCEs incorporating two distinct benzoate-based mesogenic groups, coupled with hydride-terminated poly(dimethylsiloxane). Thermomechanichal analysis of these materials revealed their exceptional capabilities as shape-memory elastomers possessing low transition temperatures [25].

Since the early 80s, patent and research activity have dealt with synthesis, characterization and properties of liquid crystalline epoxy resins. It was demonstrated that in the case of epoxies with highly crosslinked structures, superior mechanical properties, thermostability and chemical resistance were obtained [12,26–31].

In the same years, a great interest was also devoted to less densely crosslinked systems [1,2]. Barclay et al. synthesized lightly crosslinked epoxies containing the mesogens in the main chain by curing glycidyl end-capped oligoethers, based on 4,4′-dihydroxy-α-methylstilbene and α,ω-dibromoalkanes, with aromatic diamines. In this case, good mechanical orientation was obtained, however, the orientational stability above the glass temperature resulted quite poor [32].

In previous papers [2,10] some of us reported the synthesis and characterization of main-chain liquid crystalline elastomers, obtained from the curing reaction of rigid-rod mesogenic epoxy monomers with aliphatic dicarboxylic acids. It has been found that even in the case of very short rigid core such as hydroquinone, it was possible to obtain smectic network with the application of mechanical stress. This experimental evidence was related to the Landau-de-Gennes theory [2].

In order to better understand the relationship between structure and properties, a preliminary investigation on the epoxy/acid reaction mechanism is necessary. Amines are widely used as curing agents, although acids and acid anhydrides are also used for this purpose, with a predominance of the latter. Acids are preferred in some applications to amines because they give long useful pot life and they are less health hazardous. However, they have to be cured at elevated temperatures for optimum properties [33].

The reaction mechanism is more complicated than that involved in the reaction with amines [34]. According to the literature, the initial reaction expected in acid curing of epoxy resins include the addition esterification, with the formation of a hydroxy ester. The alcoholic hydroxyl would then react preferentially with epoxy groups through an etherification reaction. However, a temperature-dependent competing reaction of hydroxy ester with carboxylic acid can give rise to a condensation esterification. Besides, the addition esterification and etherification are sensitive to temperature, with higher temperatures generally favoring addition esterification and lower temperature increasing etherification [35]. The extent to which etherification will occur also depends on the nature of the carboxyl group and the location of the epoxy group in the molecule. The rate constants of the initial reaction increases with the dissociation constants of the carboxylic acids [36].

The aim of this work is to give a further insight to the relation between structure and properties exhibited by LCEs. Cross-linking reaction of epoxy monomers by means of carboxylic acids is characterized by a very complex mechanism, involving several competitive reactions, which are responsible for the dissimilar growth of the forming networks. Depending on the experimental conditions employed in the synthesis of the LC elastomers, such as nature of epoxy monomer, length of flexible spacer, curing time and temperatures, molar ratio of reactants, different physical and mechanical properties are displayed. In this framework, we prepared epoxy based LCEs obtained from two different mesogenic monomers, cured with five aliphatic dicarboxylic acids, characterized by an increasing number of methylene units. In the first part of this work, we investigated how the mechanism of growth of networks was affected by changing the type of monomer and length of flexible spacer. Furthermore, the nature of monomers and curing agents has been related to the thermodynamical parameters of cured systems, such as clearing temperatures, enthalpies and entropies, as well as to phase behavior. Since the type of response to the mechanical field is strongly structure dependent and is a major feature of LCEs, the second part of this work will deal with orientational behavior under stress, isostrain, stress–strain experiments and dynamic-mechanical experiments.

## 2. Experimental

### 2.1. Materials

Two liquid crystalline (LC) epoxy monomers, both synthesized in our laboratory, were used. Aliphatic dicarboxylic acids were employed as curing agents. Their structures are reported in Fig. 1.

#### 2.1.1. LC epoxy resins

The mesogenic monomers *p*-bis(2,3-epoxypropoxy)-α-methylstilbene (DOMS) and 4′-(2,3-epoxypropoxy)

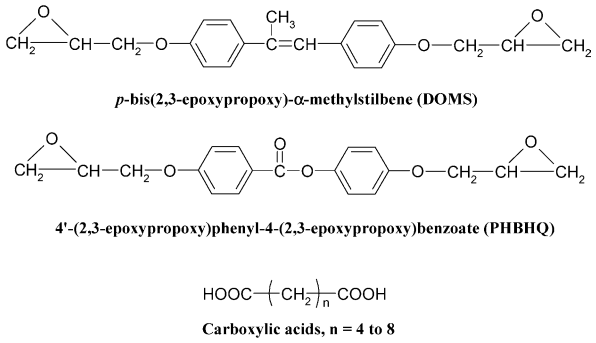


Fig. 1. Chemical structure of LC epoxy monomers and curing agents.

phenyl-4-(2,3-epoxypropoxy)benzoate (PHBHQ) were synthesized according to the procedure described in a previous paper [37]. Both epoxy compounds were recrystallized twice from ethanol/water solution. The purity of the compounds was checked by $^1$H NMR spectroscopy.

DOMS: mp = 134 °C; nematic-to-isotropic transition temperature ($T_{n\rightarrow i}$) = 115 °C, monotropic; epoxy equiv. (EEW) = 185 g/equiv.; yield = 70%. $^1$H NMR in $CDCl_3$ ($\delta$ (ppm), multiplicity, integration, attribution): 2.14, s, 3H, methyl; 2.67, dd, 2H, $CH_2$ epoxy; 2.93, dd, 2H, $CH_2$ epoxy; 3.3, m, 2H, CH epoxy; 3.9, dd, 2H, $CH_2$ glycidyl; 4.15, dd, 2H, $CH_2$ glycidyl; 6.7, s, 1H, CH on double bond; 6.8, d, 4H, CAr *ortho* to glycidyloxy; 7.3 and 7.4, m, 4H, CAr *ortho* to double bond.

PHBHQ: mp = 118 °C; $T_{n\rightarrow i}$ = 97 °C, monotropic; EEW = 180 g/equiv.; yield = 40%. $^1$H NMR in $CDCl_3$ ($\delta$ (ppm), multiplicity, integration, attribution): 2.78, m, 2H, $CH_2$ epoxy; 2.93, dd, 2H, $CH_2$ epoxy; 3.4, m, 2H, CH epoxy; 4.0, m, 2H, $CH_2$ glycidyl; 4.28, m, 2H, $CH_2$ glycidyl; 7.0, t, 4H, CAr *ortho* to glycidyloxy; 7.2, d, 2H, CAr *ortho* to ester oxygen, and 8.14, d, 2H, CAr *ortho* to carbonyl group.

### 2.1.2. Curing agents

Aliphatic dicarboxylic acids with an increasing number of methylene units (from 4 to 8) were selected as curing agents. The acids were adipic acid (AA, $n[CH_2]=4$), pimelic acid (PA, $n[CH_2]=5$), suberic acid (SubA, $n[CH_2]=6$), azelaic acid (AzA, $n[CH_2]=7$), sebacic acid (SA, $n[CH_2]=8$). All of them were purchased from Aldrich and used as received, without further purification (purity $\geq$ 98%).

### 2.1.3. Other materials

For MALDI-TOF analysis dithranol (1,8,9-anthracenetriol) and silver trifluoroacetate were used as matrix and cationizing agent, respectively. Both products were purchased from Aldrich and were used as received.

## 2.2. Curing of resins

Resins were cured by mechanically mixing the epoxy compounds and the aliphatic diacids, taken in a stoichiometric ratio (1:1). Each mixture was heated to a temperature higher than the melting points of the two components ($T$ = 135°C) and held at this temperature, under stirring, for 5 min, to make it homogeneous. Successively, it was poured between two glass slides sealed with a silicon gasket, previously treated with a surfactant agent (Surfasil®, Pierce), to be thermally cured in oven.

All samples were cured at 180 °C for 90 min. Pressure was cyclically reduced from atmospheric to 150 mmHg in order to allow degassing of samples during the cure. A differential scanning calorimetry analysis of the samples confirmed that they were completely cured.

## 2.3. Characterization

### 2.3.1. Differential scanning calorimetry (DSC)

A TA Instruments differential scanning calorimeter DSC 2920, equipped with Refrigerator Cooling System (RCS) cooling accessory, was used to monitor the curing reactions of the monomers and the phase and glass transitions temperatures of cured samples. In dynamic mode, scans were performed at 10 °C/min heating rates over a temperature range of −20 to 180 °C. In isothermal mode, the DSC was stabilized at the temperature of 180 °C, the sample readily introduced into the cell, and the experiment started. Nitrogen was used as purge gas.

### 2.3.2. Rheological measurements

Rheological measurements were performed on a Rheometric Scientific rheometer (mod. ARES), in order to assess gelation of elastomers. A dynamic time sweep test was carried out, using parallel-plate (25 mm in diameter) geometry. The temperature between plates, the oscillating frequency and amplitude were set at $T$ = 180 °C, 15 Hz, 5%, respectively. The plates were heated at the temperature of the test, and the gel point was determined as the point of crossover of the shear storage ($G'$) and loss ($G''$) moduli according to ASTM D4473 [38].

### 2.3.3. Fourier transform infrared (FT-IR) spectroscopy

The FT-IR spectroscopy was used in order to follow the curing process. FT-IR analyses were performed using a Nicolet Nexus FT-IR spectrophotometer interfaced with a Nicolet Continuμm IR microscope operated in reflectance mode. The microscope was equipped with a liquid nitrogen-cooled mercury cadmium telluride (MCT) detector and a computer-controlled translation stage (Spectra-Tech, Inc.), programmable in the $x$ and $y$ directions, equipped with a hot stage (Linkam, mod. TH 600). A film of each uncured mixture was cast onto an aluminum pan and collocated on the pre-heated hot-stage ($T$ = 180 °C). Care was taken to obtain thin and homogeneous films in order to avoid major thickness variation due to viscosity changes during gradient curing. At fixed times of the reaction, spectra were collected using 32 scans at 8 $cm^{-1}$ resolution, in the 650–4000 $cm^{-1}$ region. The ratios of the areas under the 912 $cm^{-1}$ epoxy ring peak and the 830 $cm^{-1}$ constant peak (used as an internal

standard) of the 1–4 substituted aromatic rings in the epoxy molecule, represent a relative measure of curing degree [39]: the lower the values, the higher the curing extent.

#### 2.3.4. Matrix assisted laser desorption ionisation-time of flight (MALDI-TOF)

MALDI-TOF experiments were carried out in order to monitor the molecular weight growth of the reacting systems. For this purpose, the epoxy/acid mixture was heated at $T=$ 180 °C in an oil bath under stirring, and small amounts of the reacting mixture were collected at fixed times to be analysed. Samples for MALDI analysis were prepared by mixing the analyte (a 0.1 M solution of each reacting mixture aliquot in THF), dithranol (0.2 M in THF) and silver trifluoroacetate (0.0045 M in THF), in the ratio of 1:2:1, respectively. A proper amount of this mixture was applied to the target plate to cover the 2.5 mm diameter sample position. The spot was allowed to air-dry without assistance. A Voyager DE MALDI-TOF mass spectrometer (PerSeptive Biosystems) was used in linear mode, using delayed extraction, and positive ions were examined. A 337-nm-nitrogen laser was used for sample desorption and ionization. The acceleration voltage was 22,000 volts. The low-mass cut-off was applied to reduce detector saturation by matrix and other species. The average of 100–200 laser shots were employed to obtain MALDI spectra.

#### 2.3.5. $^{1}H$ and $^{13}C$ nuclear magnetic resonance (NMR)

$^{1}H$ NMR and $^{13}C$ NMR spectra were recorded at 300 and 75.4 MHz, respectively, on a Varian Gemini 300 spectrometer with proton noise decoupling for $^{13}C$ NMR. The central peak of $CDCl_3$ was taken as reference and the chemical shifts are given in ppm from TMS using the appropriate shift conversions.

Distortionless enhancement by polarization transfer (DEPT) $^{13}C$ NMR experiments [40,41] were used in order to distinguish among the different carbon types in DOMS-SA reacting mixtures.

#### 2.3.6. X-ray diffraction

X-ray diffraction patterns were recorded by the photographic method using a Rigaku mod. III/D max generator, with a Ni-filtered Cu $K_\alpha$ radiation at room temperature. This technique was used in order to investigate the structure of LC cured material. The length of the molecular segments was calculated after energy minimization performed by means of Accelrys Cerius$^2$—3.5 release program.

## 3. Results and discussion

### 3.1. Curing reaction between epoxy monomer and carboxylic acid

#### 3.1.1. Reaction mechanism

The reaction scheme between epoxy monomer and carboxylic acids is reported in Scheme 1.

It proceeds via opening of the epoxy ring by the carboxyl group [35,42] (**1**). The hydroxyl groups produced are subsequently involved in the reaction with carboxylic acid, resulting in the formation of ester linkages by condensation (**2**), or in the etherification through the reaction with the epoxy molecules not yet reacted (**3**). On the other hand, at 180 °C, homopolymerization of the diglycidyl derivative is also a possible competitive reaction (see Scheme 2), since epoxies are reactive towards self-polymerization to polyethers [43,44].

Besides, this reaction is known as being catalysed by proton donors present in the reacting mixtures, such as carboxylic acids. The hydroxyl group in the ether dimer (**4**), can undergo both esterification with acid (**5**), or further etherification with an epoxy (**6**). Hydroxyl groups are, therefore, responsible for the formation of a lightly crosslinked network. This was confirmed by reacting epoxies and acids in the presence of inhibitors of the reaction between epoxy and hydroxyl groups, such as aromatic amines. In such conditions, only linear polymers containing hydroxyside groups were obtained [45].

The prevailing reaction path depends on the experimental conditions (reaction temperature, epoxy/acid molar ratio, nature of monomers and acids selected) and has not been clearly established [2]. In any case, independently of the monomer used, an elastomeric network was obtained.

#### 3.1.2. Thermal and rheological properties of liquid crystalline epoxy-acid mixtures

The thermal behavior of curing systems was evaluated through DSC. For this purpose, each system was subjected to an isothermal cure at 180 °C for 90 min and, subsequently, a double heating scan was carried out in order to determine any residual reactivity, the glass transition and the clearing temperatures of the cured samples. Since no residual heat was detected after isothermal cure at 180 °C for 90 min, we assumed that isothermal enthalpies could be related to the curing extent.

Table 1 reports the enthalpies calculated for the isothermal curing reactions, normalized to the effective moles of epoxy and acid units which are present, in a stoichiometric ratio of 1:1, in the reacting mixture. The molecular weight of the mixture was assumed to correspond to that of the epoxy-acid repeating unit.

A first comment is relative to the enthalpies that are constant for the PHBHQ-based systems, whereas they result lower and variable depending on the acid length in the case of DOMS. This suggests that for PHBHQ the reaction proceeds according to a different mechanism and it is less influenced by the acid length, while in the case of DOMS the reaction path is also determined by a number of side reactions whose extent is not easily predictable. The different enthalpy values may be ascribed to a lower epoxy conversion, or to the occurrence of the side reactions in different extent, characterized by different reaction enthalpies. In order to monitor the development of the

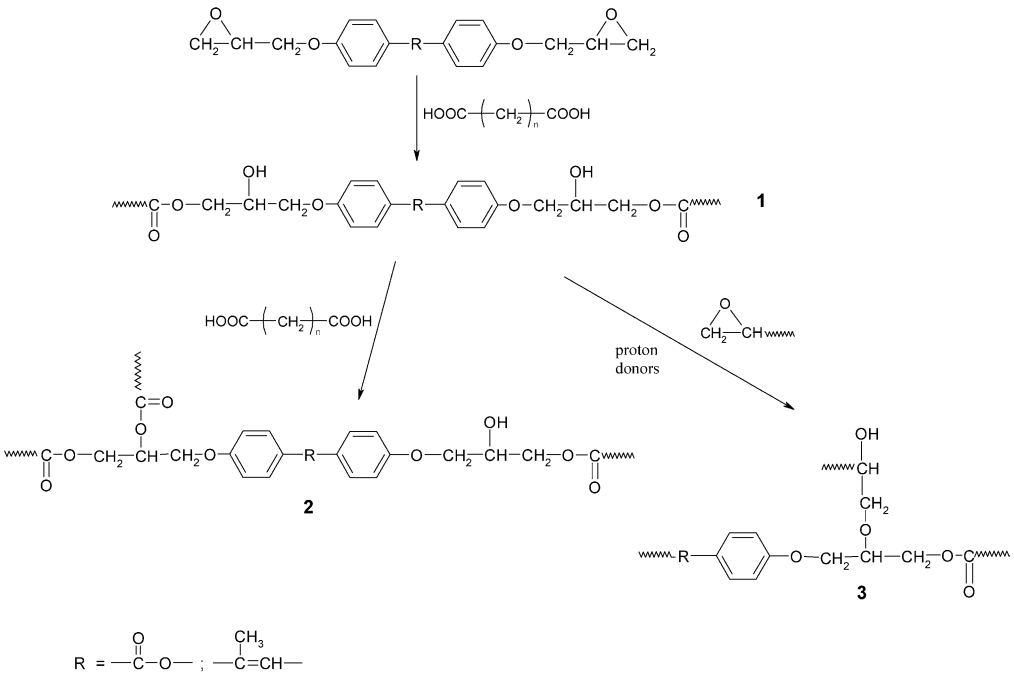


Scheme 1. Reaction scheme between epoxy monomers and carboxylic acids.

network structure, and to relate rheological changes to the reaction enthalpies obtained from DSC, rheological tests were performed on PHBHQ and DOMS cured in presence of adipic and sebacic acid. The extent of the curing reaction was related to the gel-point time. The method chosen defines the gel point as the point of crossover of the shear storage ($G'$) and the loss ($G''$) moduli in small-amplitude oscillatory shear experiments [46]. In Table 1 times and moduli at the gel-point are reported. Fig. 2(a) shows the evolution of the storage and the loss moduli at $T=180$ °C for DOMS-SA and DOMS-AA, respectively, while the results for PHBHQ-SA and PHBHQ-AA are reported in Fig. 2(b).

Initially, in the liquid state, the viscous properties are dominant, and more energy is dissipated than stored so that $G'>G''$. In the solid state, as a complete reaction is approached, the elastic properties dominate and more

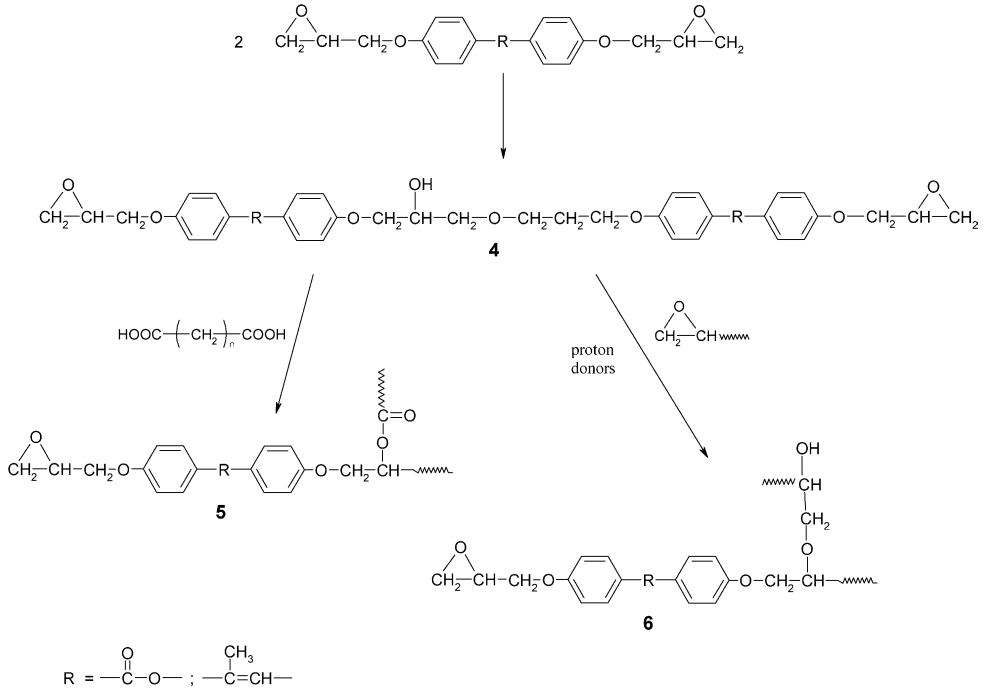


Scheme 2. Homopolymerization reaction in the epoxy/acid mixture.

Table 1
Cure enthalpies from DSC, gel times and shear moduli at gel point from rheological experiments of the mixtures based on DOMS and PHBHQ and different chain length acids

| System | $\Delta H$ cure (KJ/mol) | Time (s) | Modulus 'G' (MPa) |
|---|---|---|---|
| DOMS-AA | 41.1 | 900 | 180 |
| DOMS-PA | 96.1 | – | – |
| DOMS-SubA | 52.7 | – | – |
| DOMS-AzA | 52.6 | – | – |
| DOMS-SA | 78.3 | 1800 | 190 |
| PHBHQ-AA | 108.0 | 1400 | 830 |
| PHBHQ-PA | 108.8 | – | – |
| PHBHQ-SubA | 109.4 | – | – |
| PHBHQ-AzA | 105.0 | – | – |
| PHBHQ-SA | 107.2 | 2000 | 945 |

energy is stored than dissipated, and $G' > G''$. Consequently, the point at which $G' = G''$ may be used to define the gel time [46].

As it can be clearly seen in Table 1, for both DOMS and PHBHQ-based elastomers, the chain length of the curing agents has a great influence on gel times, while it slightly affects the moduli at the crossover point: in particular, an increase of the number of methylene units in the acids leads to higher gel times. This result may be explained in terms of capability of different chain length molecules to react to the applied shear stress, during the elastomer formation. At the beginning, the reaction between the acid and the epoxy monomer should lead to a linear product. Subsequently, during the curing process, the free volume in the growing network is reduced, resulting in a lowered mobility and an increased resin viscosity. At this point the gelation occurs and the reaction becomes diffusion controlled [47]. The nature of monomer has a clear influence also on the moduli values at the gel-point. In particular, moduli are significantly lower for DOMS systems in comparison to PHBHQ ones. This suggests that the mixtures containing DOMS react to a lower extent, although they gelify earlier, as evidenced by the reduced gel times. This is consistent with the lower curing enthalpies evaluated by DSC: the anticipated gel formation limits the diffusion of the reacting species, thus inhibiting the complete conversion of epoxy groups. DSC and rheological results suggest that, before gelification, the DOMS-based systems undergo branching during the growing of the pre-polymer chains. In order to support these hypotheses, as well as to get further insight on the reaction mechanism involved in the network formation, a combined FT-IR, MALDI-TOF and $^{1}H$ and $^{13}C$ NMR study was carried out on two selected systems, namely DOMS-SA and PHBHQ-SA.

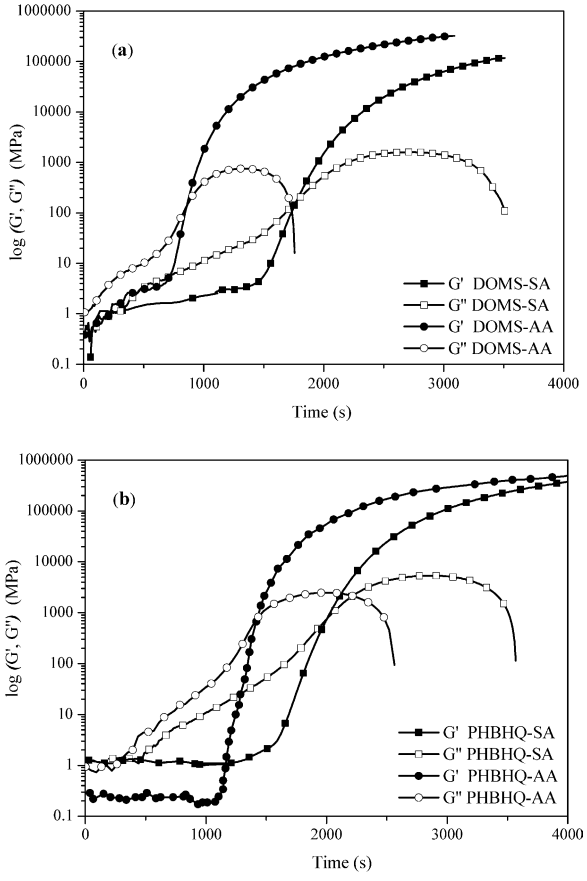


Fig. 2. Evolution of the storage ($G'$) and loss ($G''$) moduli during isothermal cure at 180 °C for (a) DOMS-SA and (b) PHBHQ-SA.

### 3.1.3. FT-IR analysis

Infra-red spectroscopy allows to monitor the amount of functional groups directly involved in the curing reaction. The relative conversion $\alpha$, of the epoxy groups in the investigated systems was determined by the usual way:

$$\alpha = \frac{C_0 - C_t}{C_0} = 1 - \frac{C_t}{C_0} \tag{1}$$

Since the experimental absorbance is low enough to be within the validity of the Beer–Lambert relation:

$$\alpha = 1 - \frac{\bar{A}_t}{\bar{A}_0} \tag{2}$$

where $C$ is the concentration, $A$ represents the absorbance, and the subscripts $0$ and $t$ denote reaction times zero and $t$, respectively. For the calculation of the relative conversion $\alpha$, peak areas have been considered instead of the peak heights. This was done in order to set more accurate calibrations, since peak areas are measured by adding the absorbance of many different data points together and are not dependent on a single data point [48]. Furthermore, $\bar{A}$ corresponds to the 912 $cm^{-1}$ peak area of the epoxy ring stretching, corrected for the sample thickness. The thickness correction was accomplished by using the invariant peak at 830 $cm^{-1}$ as an internal standard, corresponding to the out of plane =C–H bending [49].

Fig. 3 reports the relative conversion $\alpha$ for DOMS-SA and PHBHQ-SA. The extent of the epoxy ring opening reaction is lower for DOMS-SA, except for the first few

minutes, in which the conversion rate is the same for both systems. DOMS-SA system conversion rate and final extent are significantly lower than PHBHQ-SA reacting mixture. PHBHQ-SA approaches 90% of the reaction extent in 30 min, whilst DOMS-SA takes more than 60 min to reach the overall epoxy conversion extent, corresponding to 75%. If we relate these results to the values of gel times obtained from rheological analysis, it turns out that the gel time occurs at $\alpha = 64\%$ and 88% for DOMS-SA and PHBHQ-SA, respectively. Once again, experimental data suggest that the occurrence of gelation in DOMS-SA does not involve exclusively the epoxy ring opening. After gel point, when both systems have reached their 90% relative fractional conversion, the reaction becomes diffusion-controlled, inhibiting further epoxy disappearance.

Fig. 4 shows the change in absorbance corresponding to OH groups (3600–3400 $cm^{-1}$) as a function of the epoxy ring relative conversion $\alpha$. According to the reaction schemes proposed (Schemes 1 and 2) the epoxy ring opening generates new OH groups. The only reaction which leads to the net consumption of OH groups is their condensation with carboxylic acid (products **2** and **5**).

In both cases, the increase of hydroxyls is straightforward with respect to the epoxy conversion. However, in the case of DOMS-SA, for $\alpha$ values up to 0.6, the line slope is lower, suggesting that in this stage, the OH produced by the ring opening are consumed more quickly than in the case of PHBHQ-SA, as it is involved in the branching reactions. This is in agreement with the results obtained by DSC and rheological measurements. Moreover, in the case of DOMS-SA a considerable initial OH absorbance is evident, which, together with some evidences from MALDI-TOF analysis reported in the following section, led us to hypothesize that a small amount of species containing OH group, such as monoepoxy-terminated α-methylstilbene may be present. However, a reliable quantitative analysis cannot be carried out, since the alcoholic OH determination can be considerably affected by the sample and room humidity;

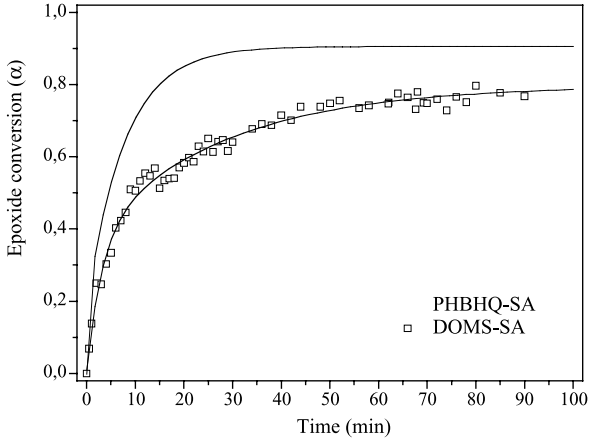


Fig. 3. Relative conversion of epoxy groups, $\alpha$, for PHBHQ-SA and DOMS-SA samples. Lines are theoretical fit of experimental data.

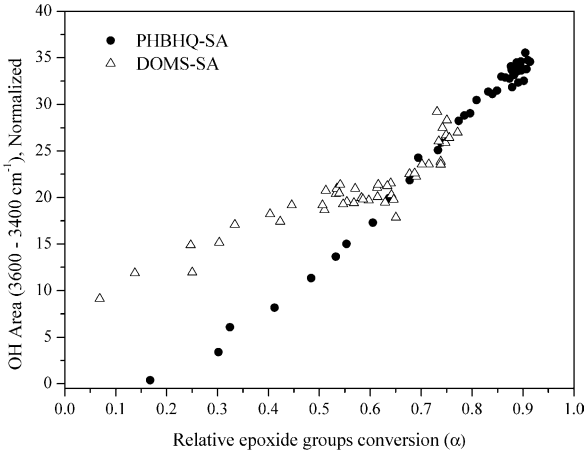


Fig. 4. Hydroxyl content (3600–3400 $cm^{-1}$) versus epoxy groups relative conversion, $\alpha$, for PHBHQ-SA and DOMS-SA samples.

furthermore, a tail of the carboxylic acid OH absorption at 3300 $cm^{-1}$ could also affect the integration of the band under examination.

### 3.1.4. MALDI-TOF mass spectrometry

In order to give a further insight on the different mechanisms involved in the network formation, MALDI-TOF spectrometry was performed on PHBHQ-SA and DOMS-SA reacting mixtures. With this method the structures and the contents of various intermediates in the reaction can be determined. In particular, in the case of epoxy resins, MALDI-TOF can be used for analyzing samples with respect to oligomer distribution and functionality. According to MALDI-TOF theory [50], the epoxy oligomers are ionized by the attachment of $Ag^+$ cations, resulting in the formation of $[M+Ag]^+$ molecular ions. However, in our experiments the presence of $Na^+$-cationized species was also found, as the preparation of reacting mixtures occurred in glass vials. During the reaction, at fixed times, small amounts of the reacting mixtures were collected and analyzed.

MALDI-TOF spectra are reported in Figs. 5 and 6 for PHBHQ-SA and DOMS-SA systems, respectively.

The epoxy resin based oligomer series can be identified by a typical peak-to-peak mass increment of the different species responsible for the growth of the systems. In particular, for PHBHQ-SA, the increment expected during the growth of the reacting system is of 342 and 202 Da, which correspond to the molecular weights of PHBHQ and sebacic acid, respectively. As for DOMS-SA concerns, the repeating unit molecular weight is 338 Da for the epoxy addition.

After 7 min of reaction, the solubility of PHBHQ-SA in THF was markedly decreased, therefore, samples suitable for MALDI-TOF analysis could not be obtained after this reaction time.

Spectra corresponding to 1, 3, 7 min of reaction are shown in Fig. 5.

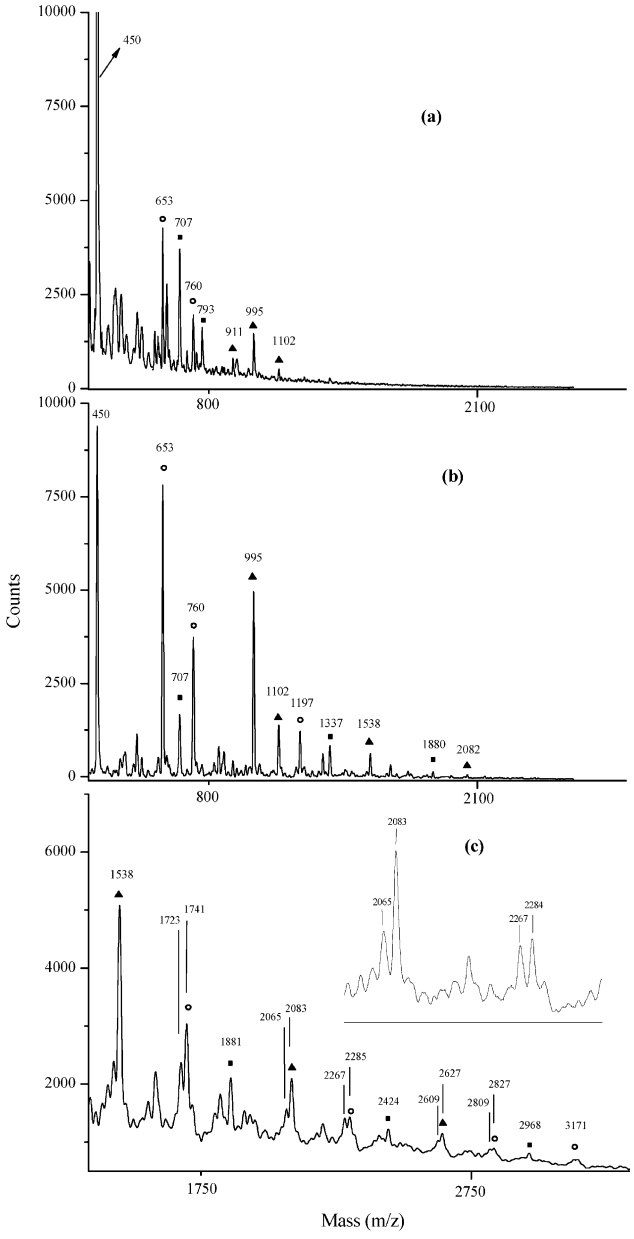


Fig. 5. MALDI-TOF mass spectra of PHBHQ-SA mixture collected during curing reaction at $T=180$ °C at (a) $t=1$ min, (b) $t=3$ min, (c) $t=7$ min.

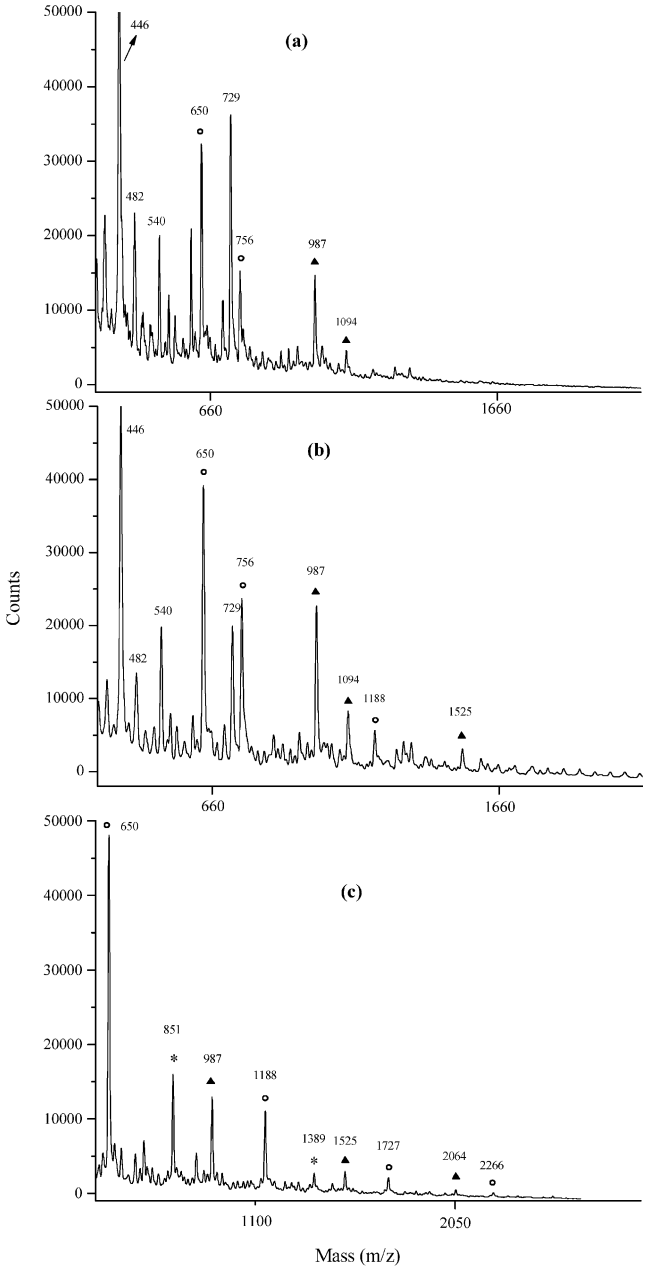


Fig. 6. MALDI-TOF mass spectra of DOMS-SA mixture collected during curing reaction at $T=180$ °C at (a) $t=1$ min, (b) $t=3$ min, (c) $t=9$ min.

At $t=1$ min the major peak ($m/z=450$) could be assigned to the adduct of pure PHBHQ/$Ag^+$. Another diagnostic peak corresponds to the species produced by the addition between the epoxy and the acid (i.e. product **1** in Scheme 1) centered at 653 $m/z$. Moreover, a peak at 760 $m/z$ was assigned to the product **1** ionized by two $Ag^+$: in this case, only one of the $Ag^+$ ions acts as a cationizing agent, whereas the other one is the counterion for the carboxylate anion. Two peaks at 707 and 793 $m/z$, corresponding to the dimer of the epoxy (i.e. product **3** in Scheme 2) cationized with $Na^+$ and $Ag^+$, respectively, are also evident. The formation of the adduct formed by one acid and two epoxy units is already noticed at this stage of the reaction, as a peak at 995 $m/z$ appears.

At $t=3$ min, the adducts corresponding to 653 and 995 $m/z$ become prevalent and new oligomers form: the peaks at 1197 and 1538 $m/z$ are representative of oligomers generated by the addition between acid and epoxy molecules in the same ratio, while at 1337 and at 1880 $m/z$ peaks corresponding to species generated by an unbalanced stoichiometry, with prevailing epoxy units, are detected.

Moreover, the reacting systems start branching through the condensation reaction between the carboxylic acid and the hydroxyl groups generated by the epoxy ring opening (products **2** and **5**). This is evidenced by the presence of

peaks exhibiting mass difference of 18 Da, due to the loss of a water molecule.

At $t=7$ min the same species pattern was detected, with a molecular weight extended up to 3200 Da.

Summarizing, in all spectra three series can be identified, characterized by a specific epoxy/acid stoichiometric ratio. Components within each series exhibit a mass difference of 544 *m/z*, which corresponds to the sum of epoxy and acid monomer molecular weights in PHBHQ-SA system. If we indicate the epoxy and the acid unit with Ep and Ac, respectively, three series can be identified, $Ep_nAc_n$ [○], $Ep_{n+1}Ac_n$ [▲], $Ep_{n+2}Ac_n$ [■],with $n$ representing the number of each unit in the oligomer.

In each series the double peaks, when present, indicate the simultaneous presence of both the addition and the condensation product, as shown in Schemes 1 and 2.

According to MALDI-TOF experiments, we can say that: in the early stage of the reaction ($t=1$ min), the acid-to-epoxy addition reaction and the homopolymerization are the prevailing reactions in the PHBHQ-SA system. Subsequently, species with prevailing epoxy units ($Ep_{n+1}Ac_n$, $Ep_{n+2}Ac_n$) are observed. No evidence of species containing an excess of acid units was found. Branching accompanied with loss of water starts occurring after $t=3$ min.

In the case of DOMS-SA, samples up to 15 min reaction could be analyzed. In Fig. 6 spectra corresponding to 1, 3, 9 min of reaction are shown.

The major peaks are representative of species of the same typology ($Ep_nAc_n$, $Ep_{n+1}Ac_n$, $Ep_{n+2}Ac_n$) of PHBHQ-SA system. However, only traces of epoxy dimers are evident and numerous by-products are responsible for more complex spectra. Branching through the reaction between hydroxyl groups and acid molecules, involving the loss of water occurs only at $t=9$ min, and peaks corresponding to condensation products are barely distinguishable throughout all the spectra, suggesting a lower occurrence of this pathway when compared to PHBHQ-SA during the first 15 min of reaction (i.e. up to about 50% epoxy conversion). In addition, the maximum molecular weight detected is 2267 Da, even at $t=15$ min, corresponding to the addition product of 4 epoxy and 4 acid units. These results matched the FT-IR evidences, as the epoxy conversion for DOMS-SA is lower than PHBHQ-SA units.

An evident feature of DOMS-SA spectra is the appearance of unexpected peaks. In particular, at $t=1$ min peaks at 389 and 729 *m/z* may be attributed to species containing monoepoxy-terminated molecules. The presence of monoepoxy-terminated DOMS in the synthesized compound was not indeed revealed by NMR (see Section 2.1.1), but this may be due to the poor solubility of such compound in chloroform, which was used as a solvent in NMR experiments. Furthermore, the peaks at 851 and 1389 *m/z* become significant at $t=9$ min. This mass values are representative of oligomers with prevailing acid units ($Ep_nAc_{n+1}$ [*], Fig. 6), which did not undergo condensation reaction. Since these species were not found in PHBHQ-SA spectra, it is unlikely that they correspond only to the conventional addition products to the epoxy groups, suggesting an alternative pathway of reaction between acid and epoxy.

### 3.1.5. NMR analysis

Differences between the growth mechanisms of PHBHQ-SA and DOMS-SA depend on the different reactivity of the starting epoxy molecule: that is, in the case of DOMS, some other side reactions, different from the case of PHBHQ-SA, as inferred from MALDI-TOF analysis, must be taken into account. In order to investigate this, $^{13}C$ and $^{1}H$ NMR analyses were performed in deuterochloroform on the reacting DOMS-SA systems, at reaction time $t=0$ and 15 min, respectively.

The stoichiometric mixture was prepared by mechanically mixing the two components and heating them at 135 °C under stirring for 5 min, as described in the experimental part; a sample was taken from the vial at this time, which was considered as the initial reaction time ($t=0$). Then, the remaining mixture was put in a thermostatic bath at 180 °C for 15 min and subsequently fastly cooled in an ice bath in order to stop the reaction at this time.

Fig. 7 reports the $^{13}C$ spectrum between 0 and 200 ppm of DOMS-SA mixture at $t=0$. DEPT experiments allowed us to distinguish among primary and tertiary, secondary, and quaternary carbon atoms. The signal attribution was performed with the aid of the spectra of the pure starting compounds and by comparison with the expected chemical shifts obtained by means of empirical calculations [51]. The detailed attributions are reported in Table 2 and Fig. 8, respectively.

The presence of three aromatic signals between about 126 and 132 ppm was attributed to a mixture of *cis* and *trans* isomers for pure DOMS. Two unexpected peaks at 34 and 100 ppm, respectively, were found. Their presence was attributed to the addition of the carboxylic acid to the central double bond of DOMS. In fact, in the presence of acidic hydrogens, the central double bond of the mesogen can give rise to a stabilized benzyl carbocation, which can subsequently catalyze the epoxy group homopolymerization or undergo addition of the carboxylate (Scheme 3) [52]. Therefore, we deduced that this reaction occurs even at $t=0$ (i.e., when the sample has been heated 5 min at 135 °C under stirring, while in the molten state). The amount of addition to the double bond could be estimated by means of the $^{1}H$ NMR spectrum of the mixture at $t=0$ (Fig. 9).

We compared the integration of the peak at 2.14 ppm, which corresponds to the protons of the methyl group on the double bond, with the integration of the peak at 1.15 ppm, which can be attributed to the protons of the methyl group in the addition product; from this comparison, it resulted that the amount of reaction is lower than 15% in these conditions.

Fig. 10 reports the $^{13}C$ NMR spectrum, magnified between 0 and 104 ppm, of DOMS-SA reacted 15 min at

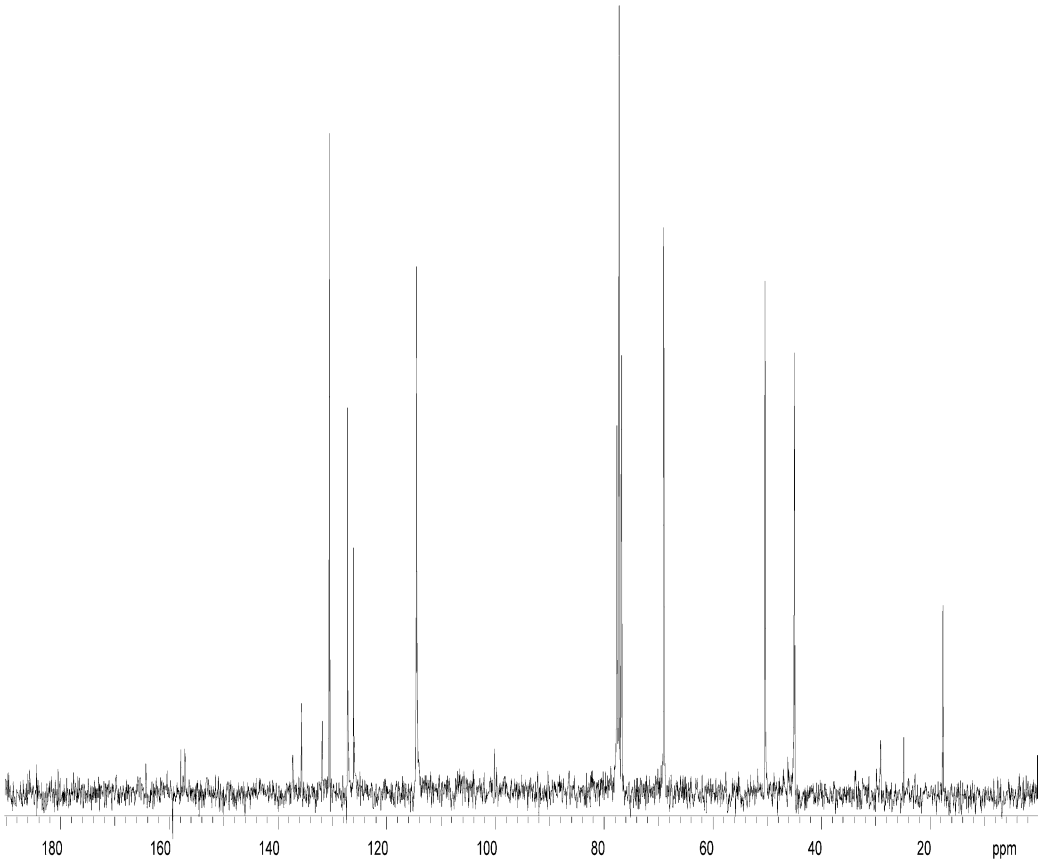


Fig. 7. $^{13}C$ NMR spectrum between 0 and 200 ppm in $CDCl_3$ of DOMS-SA mixture at $t=0$.

180 °C. As expected, in addition to the signals already observed at $t=0$, the signals ascribed to the opening of the epoxy group by reaction with the acid, appear at 62.08, 65.18 and 66.28 ppm, respectively; furthermore, very small peaks at about 72.6 and 78 ppm were attributed to the opening of the epoxy group in the homopolymerization reaction [53].

Table 2
Signal attribution of $^{13}C$ NMR spectrum in $CDCl_3$ of the reaction mixture DOMS-SA at $t=0$ C* and C§ are Ca and Cc, respectively, after reaction with SA

| Chemical shift (ppm), and carbon type | Attribution (see also Fig. 8) |
|---|---|
| 17.41, primary | Cb |
| 24.60, secondary | C2′ |
| 28.93, secondary | C4′, C5′ |
| 34.10, secondary | C§ |
| 44.74, secondary | C3 |
| 50.17, tertiary | C2 |
| 68.81, secondary | C1 |
| 100.01, quaternary | C* |
| 114.32, tertiary | Aromatic CI and CII |
| 125.90, 127.00 and 131.66, tertiary | Aromatic CIII and CIV (unreacted DOMS) |
| 127.26, tertiary | Aromatic of reacted DOMS |
| 130.37, tertiary | Cc |
| 135.48, quaternary | Ca |
| 137.10, quaternary | CV |
| 156.97, quaternary | CVI |
| 164.16, quaternary | Carbonyl group |

$^1H$ NMR spectrum (Fig. 11) carried out on samples that reacted for 15 min shows many unresolved peaks due to the presence of many products as well as to the starting compounds and it is, therefore, complicated to interpret in detail. Also, for this reason we could not correctly integrate the peak attributed to the protons of the methyl group in the addition product, which lies in an unresolved peak centred at about 1.20 ppm: therefore, this prevented us from

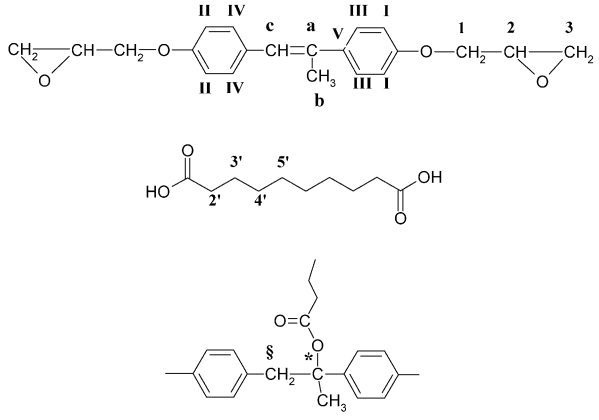


Fig. 8. Products and relative attribution of the signals observed by $^{13}C$ NMR experiments for the reaction mixture DOMS-SA at $t=0$.

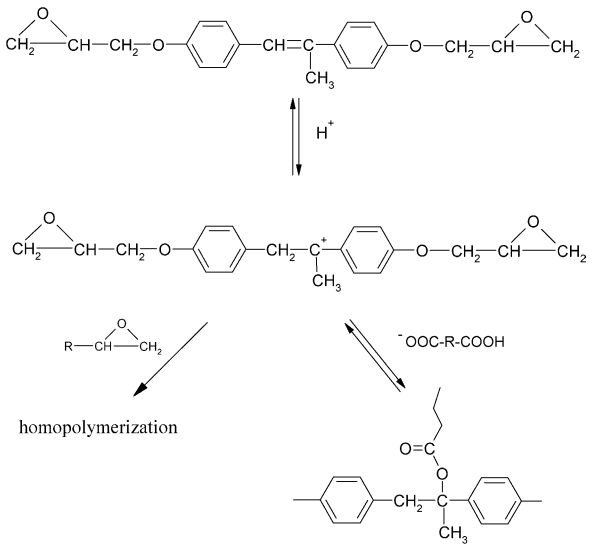


Scheme 3. Formation of benzyl carbocation and its subsequent reactions for DOMS in the presence of carboxylic acids.

estimating the extent of addition of the acid to the central double bond of DOMS in the mixture that reacted for 15 min. Anyway, we can reasonably suppose that this reaction remains minimal as it would destroy the rigid core of DOMS, which is responsible for liquid crystallinity. However, the addition of the acid to the double bond can be considered a reasonable explanation of the differences between DOMS-SA and PHBHQ-SA shown by the rheological tests, FTIR and MALDI-TOF: DOMS-SA system grows more branched and irregularly compared with PHBHQ-SA. This implies a lower conversion degree of the epoxy group, because part of the acid has reacted with the central double bond. For PHBHQ-SA, the growth occurs mainly as a consequence of the acid addition to the epoxy group and branching occurs when epoxy and carboxylic groups react with the hydroxyl groups. Furthermore, as evidenced by MALDI-TOF analysis, the molecular weight of DOMS-SA increases more slowly and oligomers with prevailing acid units, which do not undergo condensation reaction, are present. Finally, lower gel times can be expected for DOMS-SA if we imagine that, in this system, branched oligomers can be easily crosslinked and turn into microgels.

### 3.2. Characterization of cured LC systems

#### 3.2.1. Thermal properties of LC elastomers

LC epoxy monomers cured with aliphatic diacids produce flexible networks upon cure. This means that chain segments between crosslinks are still able to move freely and, in the case of LC systems, can give rise to a LC-to-isotropic transition at temperatures above $T_g$s. In the case

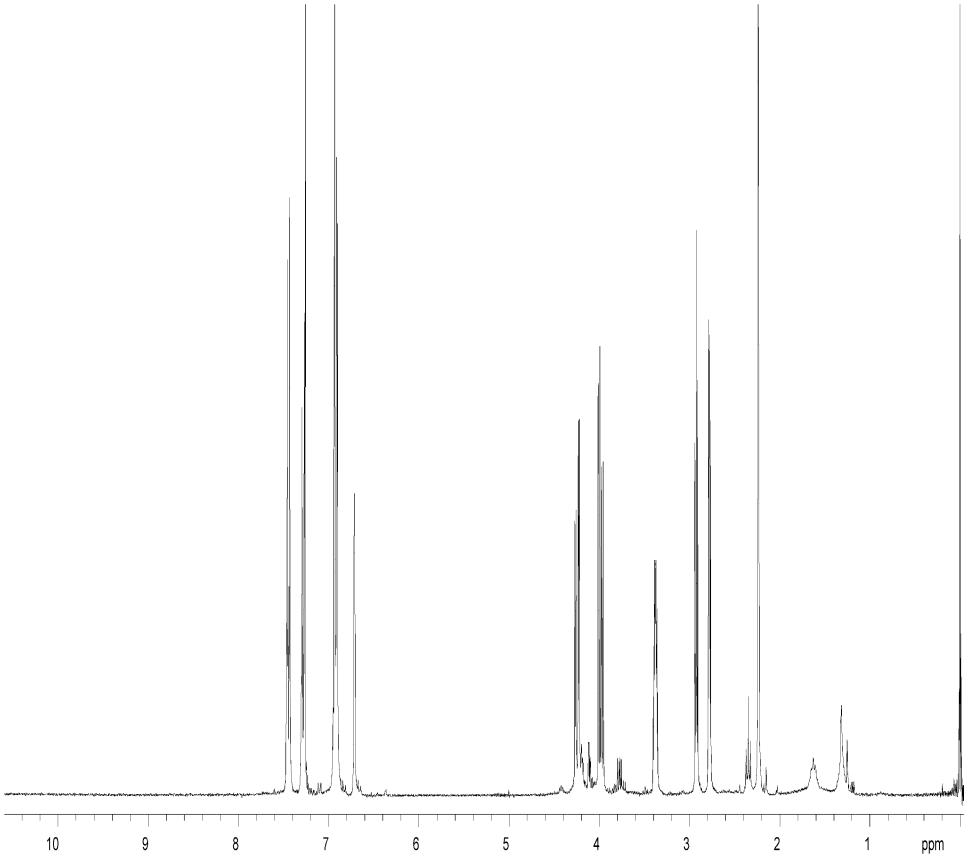


Fig. 9. $^1$H NMR spectrum in $CDCl_3$ of DOMS-SA mixture at $t=0$.

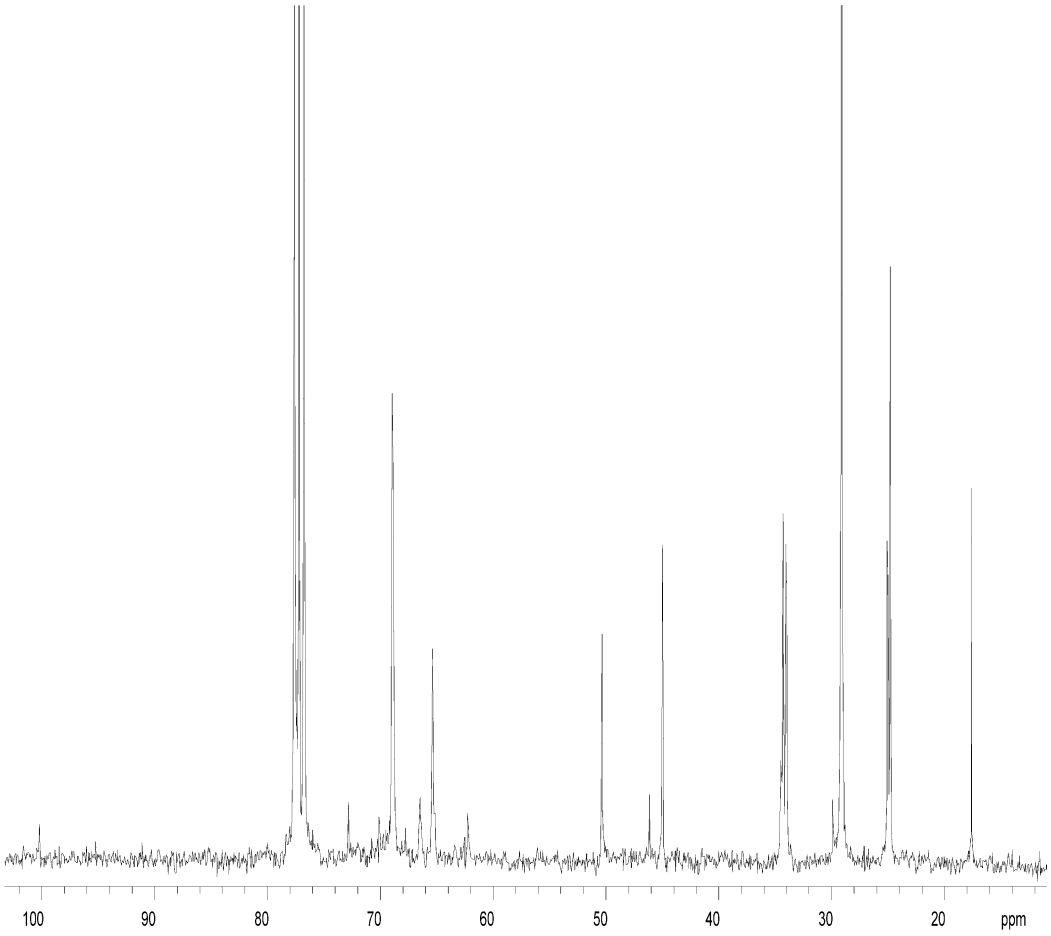


Fig. 10. $^{13}C$ NMR spectrum in $CDCl_3$, magnified between 0 and 104 ppm, of DOMS-SA mixture reacted 15 min at 180 °C.

of PHBHQ- and DOMS-derived systems, DSC put into evidence, along with the glass transition, an endothermic peak, which corresponded to LC-to-isotropic phase transition, as it was inferred from the polarized light optical microscopy observation of heated samples. The nature of the mesophase was established by means of X-ray diffraction (XRD) experiments, which are described in Section 3.2.2.

Glass transition, clearing temperatures ($T_g$s) for cured systems obtained from DOMS, PHBHQ and different aliphatic diacids ($n=4$–8) are listed in Table 3, together with the clearing enthalpies and entropies. Data were inferred from DSC second heating scans. Data are normalized with respect to a theoretical unit formed by an epoxy molecule plus an acid molecule.

The phase diagrams of the systems are reported in Fig. 12. The chain length of diacids does not affect significantly the glass transition temperatures of elastomers containing the same epoxy monomer. The clearing temperatures do not show any remarkable odd–even effect in their trend, for both PHBHQ and DOMS systems.

Smectic elastomers formed even with acids with short aliphatic chain, such as adipic acid, in the case of DOMS, as it was inferred from XRD. On the other hand, in the presence of PHBHQ, a smectic phase was observed only for $n>5$, whereas networks with shorter aliphatic units showed nematic behaviour. If one considers that the starting epoxy monomers do not exhibit a thermodynamically stable mesophase, this means that both the aliphatic segments, and the hydrogen bonds, which are formed upon cure, play a fundamental role in the development and subsequent stabilization of the mesophase.

Fig. 13 reports the clearing enthalpy versus number of methylene groups in the acids, for DOMS and PHBHQ systems, respectively. Data were fitted in the case of smectic systems, i.e. for all the acids used in the case of DOMS and for a number of methylene units between 6 and 8 in the case of PHBHQ. When the enthalpy or the entropy of transition is plotted versus the number of units in a flexible spacer, the intercepts and the slopes of the resulting linear lines are the respective contributions of mesogen order and spacer order changes at the transition. This method was developed by different authors, in thermotropic liquid crystalline polymers having spacing of different lengths [54–56]. Its applicability to the systems under examination only aims to a qualitative evaluation of the stabilizing effect of the aliphatic portion, as our systems are lightly crosslinked and, especially in the case of DOMS, are originated by a still

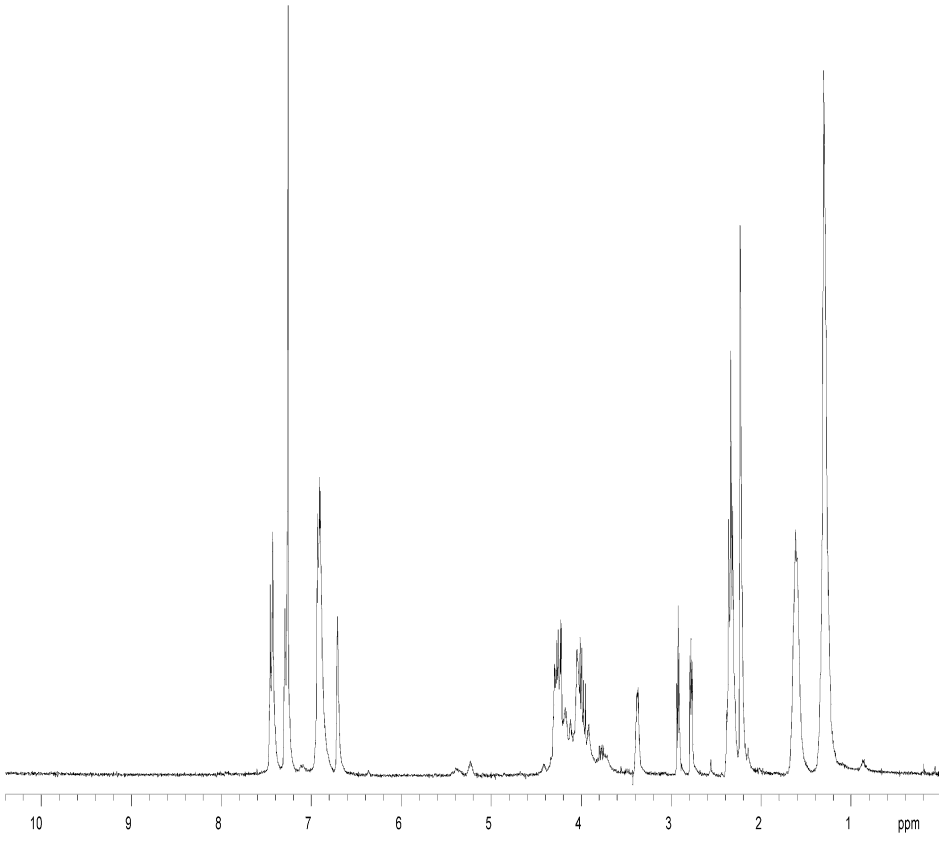


Fig. 11. $^{1}$H NMR spectrum in $CDCl_3$ of DOMS-SA mixture reacted 15 min at 180 °C.

unclear reaction path; moreover, as mentioned above, it is reasonable to suppose that, for these networks, hydrogen bonds also play a positive role in the stabilization of the mesophase [2,57]. Surprisingly, the straight lines obtained in the case of PHBHQ and DOMS, respectively, have the same slope although these systems were found to grow in a different way: that is, the aliphatic portions seem to stabilize the mesophase at the same extent in the two systems. In both cases, the intercept corresponds to a negative value of enthalpy, i.e. clearing would be thermodynamically favoured in the absence of methylene groups, which is coherent with the monotropic nature of both epoxy monomers.

### 3.2.2. X-ray diffraction analysis

Wide-angle X-ray diffraction performed at room temperature was used to identify the mesophase of the different systems synthesized. Since all LC elastomers are characterized by a low degree of cross-linking they can be oriented by tensile elongation. This phenomenon is a well-known property of both main-chain and side-chain LCEs: when deformed in tension, the LC domains elongate and rotate their local director along the tensile axis to form a 'liquid single crystal' [4,58]. Depending on the material and on the external conditions, one can obtain samples of nematic and smectic phases that are without preferred orientation ('polydomains'), samples with moderate preferred

Table 3
Glass transition and clearing temperatures, enthalpies and entropies for cured systems obtained from DOMS, PHBHQ and different aliphatic diacids, calculated by DSC second heating scan

| System | $T_g$ (°C) | $T_i$ (°C) | $\Delta H_i$ (KJ/mol) | $\Delta S_i$ (J/mol K) |
|---|---|---|---|---|
| DOMS-AA | 33 | 67 | 3.3 | 9.7 |
| DOMS-PA | 31 | 58 | 4.0 | 12.1 |
| DOMS-SubA | 26 | 63 | 7.3 | 21.7 |
| DOMS-AzA | 32 | 69 | 12.6 | 36.8 |
| DOMS-SA | 30 | 80 | 15.0 | 42.5 |
| PHBHQ-AA | 37 | 61 | 0.083 | 0.25 |
| PHBHQ-PA | 32 | 52 | 0.17 | 0.52 |
| PHBHQ-SubA | 30 | 56 | 2.3 | 7.00 |
| PHBHQ-AzA | 29 | 55 | 5.6 | 17.1 |
| PHBHQ-SA | 36 | 87 | 9.5 | 26.4 |

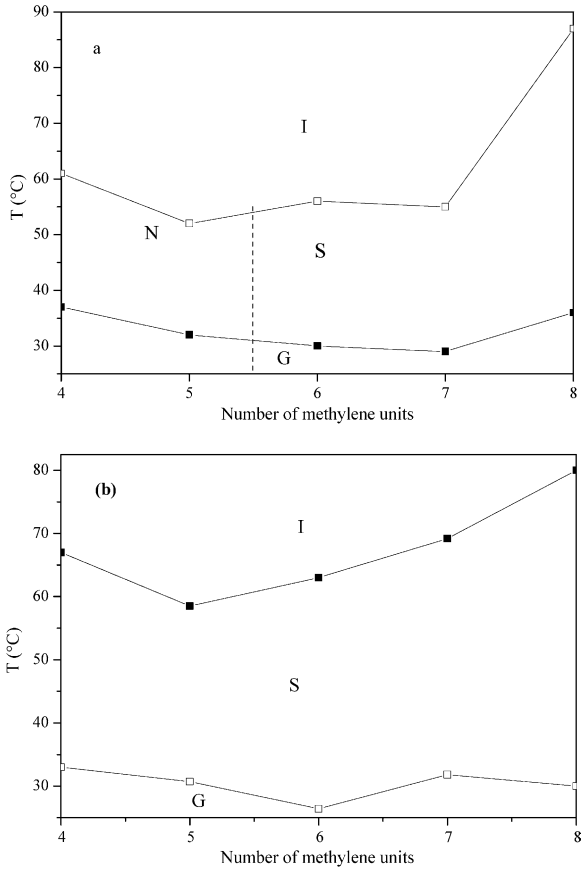


Fig. 12. Phase diagrams based on DSC data of the acid cured (a) PHBHQ and (b) DOMS systems.

orientation or samples with strong preferred orientation ('monodomains'). As a representative example, the X-ray patterns of PHBHQ-AzA, taken at room temperature, are shown at different strain values ($\Delta l/l_0 = 0$ and 4.7, respectively) (Fig. 14).

The X-ray pattern showed, for $\Delta l/l_0 = 0$ (Fig. 14(a)), a diffuse wide-angle halo, indicating a disordered arrangement of mesogenic units. From the diameter of the outer maxima, calculations of the average intermolecular distance, $D$, i.e. the average distance between the long axes of adjacent molecules, can be done. The inner diffraction ring is indicative of a smectic phase. In smectic phases, a stack of identical flat layers, parallel to each other, can be identified. In such phases, the inner maxima are related to the spacing of the smectic layers, $d$. At this point the sample is opaque, indicating the existence of a 'polydomain' microstructure.

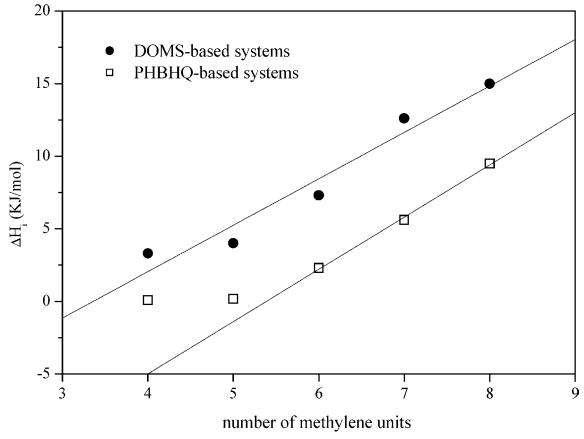


Fig. 13. Clearing enthalpy versus number of methylene groups in the carboxylic acids, for acid cured PHBHQ and DOMS systems. In the case of PHBHQ the linear fit was performed only on smectic systems ($n[CH_2] = 6$–8.

The X-ray pattern of the sample stretched ($\Delta l/l_0 = 4.7$) in the rubbery state and subsequently quenched to the glassy state (Fig. 14(b)) shows a broadened wide-angle reflection at the equator, while the smectic layer reflections can be observed at the meridian, indicating a perpendicular orientation of the smectic layer to the stress direction. Moreover, the imaginary line connecting the outer maxima is perpendicular to the one connecting the centers of the inner maxima. Therefore, the direction of the smectic layers results perpendicular to the rigid rods, thus indicating a smectic phase of type A [59]. As a consequence of the strain, the sample underwent a polydomain-to-monodomain transition and became transparent. The sharpness of outer maxima give information on the orientation of the director: a sharp maximum indicates an ordered packing and a broad maximum indicates disordered packing [59]. In particular, in the case of a monodomain, the intensity of the outer ring allows to calculate the orientational order parameter $S$. The calculation of $S$ as well as the orientational behavior of the systems under investigation are the object of Part 2 of this paper.

Mesophases and typical spacing values of unstressed elastomers were determined by XRD, at room temperature, and listed in Table 4.

PHBHQ-based systems cured with adipic and pimelic acids exhibited nematic structure. As the number of methylene units increased, X-ray patterns showed a sharp inner diffraction ring at spacings typical of a smectic molecular organization. As for the systems containing DOMS, they were all characterized by a smectic structure.

For smectic samples, layer thickness, $d$, increased with increasing acid chain lengths. The trend for both PHBHQ and DOMS-based systems is reported in Fig. 15.

As it can be noticed, the length of the aliphatic portion contributes to the smectic layer thickness at the same extent in both systems, despite the differences in the growth mechanism previously shown. A very simplified modelling, which could help us hypothesize how the smectic layer is formed, was performed by means of Accelrys Cerius$^2$—3.5 release software. We considered oligomers formed by each of the two different mesogens endcapped on both sides with acid units (Fig. 16).

The carboxylic group farther from the mesogenic core was converted into methyl ester in order to eliminate the strong interactions which would establish due to free –COOHs and to approximate in as accurate as possible way

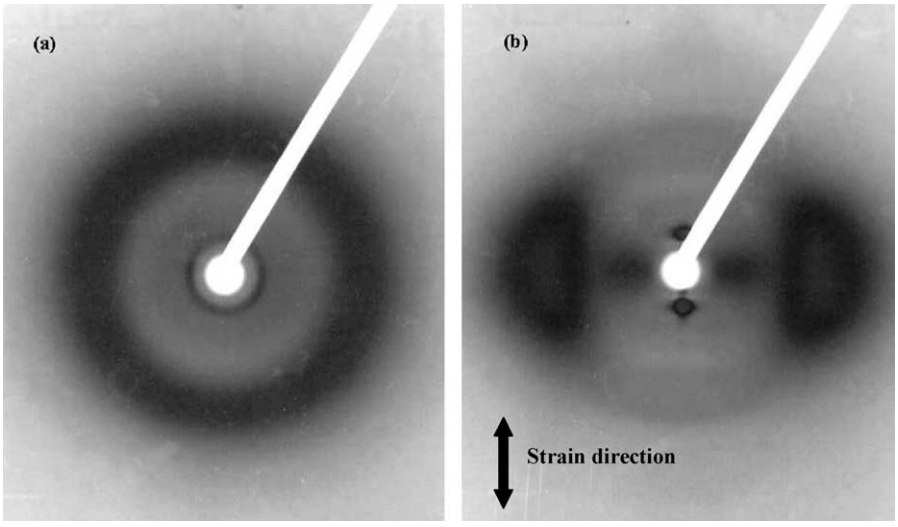


Fig. 14. X-ray patterns of PHBHQ/AzA sample at (a) $\Delta l/l_0=0$ and (b) $\Delta l/l_0=4.7$. The arrow indicates the strain direction.

the 'real' situation, where the polymeric chain is attached to the carboxylic group. Then, we performed conformer analysis by randomly sampling the conformers and assigning a 30° window for the torsion angles of different carbon sequences of both aliphatic chains. We then minimized the energy of the conformers, sampled in this way, by means of the Universal Force Field. Finally, we measured the distances of different points (i.e., between carbonyl groups, between hydroxyls, etc.) of the oligomers, which had the lowest energy values. In this model, we suppose that the polymeric portions, consisting of alternating mesogenic and aliphatic moieties, are involved in the formation of the smectic layers. Therefore, the layer thickness $d$ could approximately correspond to the distance between the carbon 2 (see Fig. 16) in the case of the systems obtained by reaction of acids with shorter aliphatic chains (i.e. $n=4$–6); on the other hand, in the case of reaction with longer acids, ($n=7,8$) $d$ seems to be better approximated by the distance between the carbons **1**. In fact, if we consider (Fig. 16), for example, DOMS-AA system, the experimental $d$ is 12.3 Å and the value calculated by Cerius[2] is 12.2 Å; for PHBHQ-SubA, $d$ is 14.6 Å and the calculated value is 14.4 Å; for PHBHQ-SA, $d$ is 16.6 Å and the calculated value is 16.6 Å; for DOMS-SA, $d$ is 16.2 Å and the calculated value is 15.1 Å. Of course, the performed modelling is extremely far from the real situation, where a number of factors strongly affect the molecular organization: Van der Waals interactions between polymeric portions, steric hindrance, interactions between mesogenic cores, distortions caused by crosslinks, etc. The proposed model must be, therefore, considered a simple preliminary hypothesis of the system organization, and deserves further, more accurate investigation.

Table 4
Calculated spacings ($D$ and $d$) and nature of mesophase of cured LC elastomers; N and $S_A$ stand for nematic and smectic A, respectively

| LC system | Mesophase | Spacings (Å) | |
|---|---|---|---|
| | | $D$ | $d$ |
| PHBHQ-AA | N | 4.5 | – |
| PHBHQ-PA | N | 4.5 | – |
| PHBHQ-SubA | $S_A$ | 4.5 | 14.6 |
| PHBHQ-AzA | $S_A$ | 4.9 | 15.7 |
| PHBHQ-SA | $S_A$ | 4.9 | 16.6 |
| DOMS-AA | $S_A$ | 4.3 | 12.3 |
| DOMS-PA | $S_A$ | 4.3 | 13.4 |
| DOMS-SubA | $S_A$ | 4.2 | 14.3 |
| DOMS-AzA | $S_A$ | 4.2 | 15.2 |
| DOMS-SA | $S_A$ | 4.2 | 16.2 |

## 4. Conclusions

In this paper, the properties of LC elastomers were studied by taking into account the different nature of epoxy monomers and curing agents. Experimental results

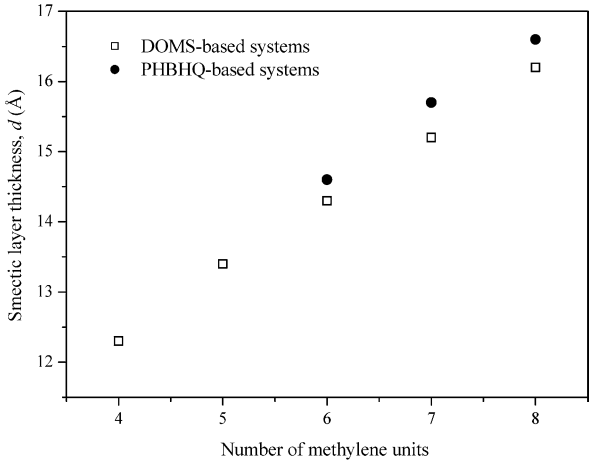


Fig. 15. Layer thickness $d$ in the unoriented smectic samples versus number of methylene units, $n$, contained in the carboxylic acids used as curing agents.

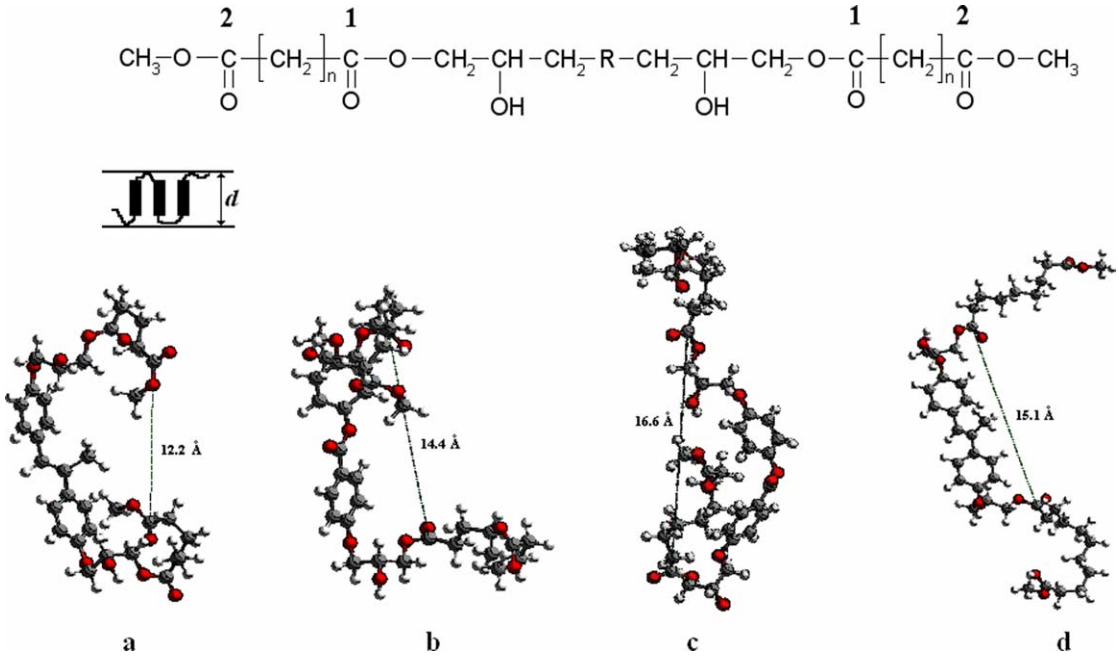


Fig. 16. Hypothesized arrangement and calculated thickness *d* of the smectic layers for (a) DOMS-AA, (b) PHBHQ-SubA, (c) PHBHQ-SA, (d) DOMS-SA.

suggested that the systems containing DOMS develop in a more complex way if compared to those based on PHBHQ. MALDI-TOF results indicated that DOMS-based systems, when compared to those containing PHBHQ, reached a lower molecular weight before the formation of an insoluble gel. Moreover, the epoxy group conversion occurred in minor extent in the case of DOMS. This can be explained with a higher extent of side reactions occurrence. Among them, the one involving the formation of a carbocation intermediate, as inferred from NMR experiments, must be taken into account. Rheological measurements indicate that the nature of starting epoxy monomer and the number of methylene units in the dicarboxylic acids play an important role on the gel point. In particular, moduli at gel time depend on the monomer used whereas a little effect is due to the acid length, while an increase of the number of methylene units in the curing agent leads to higher gel times. Besides, the occurrence of side reactions responsible for the higher extent of branching in DOMS systems leads to anticipated gel-times.

The DSC and X-ray diffraction analyses allowed us to determine the clearing temperatures, enthalpies and entropies and the nature of phases exhibited by unstrained elastomers. It was found that the mesophase is stabilized not only by the rigid segment in the epoxy monomers, but also by the aliphatic portions of carboxylic acids. Furthermore, the polydomain-to-monodomain transition was found to occur upon stretching of all the LCEs. The investigation carried out on curing mechanism and its influence on network structure is an essential step to explain the mechanical and dynamic-mechanical properties of LCEs. The second part of this work will deal with dynamic-mechanical, isostrain and stress–strain experiments performed on the cured systems.

## Acknowledgements

The authors would like to thank Ramón Guerrero for his help in performing NMR experiments. The paper was prepared with partial financial support from University and Research Italian Minister (MIUR-COFIN 2003).

## References

[1] Ortiz C, Wagner M, Bhargava N, Ober CK, Kramer EJ. Macromolecules 1998;31:8531–9.
[2] Giamberini M, Amendola E, Carfagna C. Macromol Chem Phys 1997;198:3185–96.
[3] Finkelmann H, Koch HJ, Rehage G. Makromol Chem Rapid Commun 1981;2(4):317–22.
[4] Küpfer J, Finkelmann H. Makromol Chem Rapid Commun 1991; 12(12):717–26.
[5] Hess M. In: Brostow W, editor. Performance of plastics. Munich: Hanser; 2000 [chapter 21, and references therein].
[6] Mitchell GR, Davis FJ, Guo W. Phys Rev Lett 1993;71(18):2947–50.
[7] ten Bosch A, Varchon L. Macromol Theory Simul 1994;3:533–42.
[8] de Gennes PG. Phys Lett A 1969;28(11):725–6.
[9] Zentel R. Prog Colloid Polym Sci 1987;75:239–42.
[10] Giamberini M, Amendola E, Carfagna C. Macromol Rapid Commun 1995;16:97–105.
[11] Hoyt AE, Benicewicz BC, Huang SJ. Polym Prepr 1989;30(2):536–7.
[12] Ortiz C, Kim R, Rodighiero E, Ober CK, Kramer EJ. Macromolecules 1998;31:4074–88.
[13] Kaufhold W, Finkelmann H. Makromol Chem 1991;192(11): 2555–79.
[14] Schäzle J, Kaufhold W, Finkelmann H. Makromol Chem 1989; 190(12):3269–84.
[15] Landau L. Phys Z Sowjetunion 1937;11:26–47.
[16] de Gennes PG. Mol Cryst Liq Cryst 1971;12:193–214.
[17] Thomsen III DL, Keller P, Naciri J, Pink R, Jeon H, Shenoy D, et al. Macromolecules 2001;34:5868–75.

[18] Hirschmann H, Roberts PMS, Davis FJ, Guo W, Hasson CD, Mitchell GR. Polymer 2001;42(16):7063–71.
[19] Clarke SM, Hotta A, Tajbakhsh AR, Terentjev EM. Phys Rev E 2001; 64(6–1):061702/1–061702/8.
[20] Zanna JJ, Stein P, Marty JD, Mauzac M, Martinoty P. Macromolecules 2002;35(14):5459–65.
[21] Jia YG, Zhang BY, Tian M, Pan W. J Appl Polym Sci 2004;93(4): 1736–42.
[22] Zentel R, Reckert G. Makromol Chem 1986;187(8):1915–26.
[23] Percec V, Kawasumi M. Macromolecules 1991;24(23):6318–24.
[24] Bergmann GHF, Finkelmann H, Percec V, Zhao M. Macromol Rapid Commun 1997;18:353–60.
[25] Rousseau IA, Mather PT. J Am Chem Soc 2003;125(50):15300–1.
[26] Mueller HP, Gipp R, Heine H. Ger Patent N. 36,22,610; 1986.
[27] Dhein R, Mueller HP, Meier HM, Gipp R. Ger Patent N. 36,22,613; 1986.
[28] Morgan RJ, Mones ET, Steele WJ. Polymer 1982;23:295–305.
[29] Jahromi S, Kuipers WAG, Norder B, Mijs WJ. Macromolecules 1995; 28(7):2201–11.
[30] Carfagna C, Amendola E, Giamberini M. Prog Polym Sci 1997;22: 1607–47.
[31] Carfagna C, Amendola E, Giamberini M, Filippov AG. Makromol Chem 1994;195:279–87.
[32] Barclay GG, McNamee SG, Ober CK, Papathomas KI, Wang DW. J Polym Sci, Part A 1992;30(10):1845–50.
[33] Mika TF, Bauer RS. Curing agents and modifiers. In: May CA, editor. Epoxy resins, chemistry and technology. New York: Marcel Dekker; 1988, p. 483.
[34] Matejka L, Pokorný S, Dušek K. Makromol Chem 1985;186:2025–36.
[35] Lee H, Neville K. Handbook of epoxy resins. New York: McGraw Hill; 1967 [chapter 11].
[36] Tanaka Y, Bauer RS. Curing reactions. In: May CA, editor. Epoxy resins, chemistry and technology. New York: Marcel Dekker; 1988, p. 285.
[37] Giamberini M, Amendola E, Carfagna C. Mol Cryst Liq Cryst 1995; 266:9–22.
[38] ASTM D 4473-03. Standard test method for plastics: dynamic mechanical properties: cure behavior. ASTM International; 2003.
[39] Lee JY, Shim MJ, Lee HK, Kim SW. J Appl Polym Sci 2001;82: 2372–80.
[40] Morris GA. In: Levy GC, editor. Pulsed methods for polarization transfer in carbon-13 NMR. Topics in $^{13}$C NMR spectroscopy, vol. 4. New York: Wiley; 1984. p. 179–96.
[41] Bendall MR, Doddrell DM, Pegg DT, Hull WE. DEPT Bruker Analytische Messtechnik, Karlsruhe; 1982.
[42] Saunders KJ. Organic polymer chemistry. New York: Chapman and Hall; 1988, p. 412–427.
[43] Galià M, Mantecon A, Càdiz V, Serra A. Makromol Chem 1990;191: 1111–8.
[44] Wang MS, Pinnavaia TJ. Chem Mater 1994;6:468–74.
[45] Hirn B, Carfagna C, Lanzetta R. J Mater Chem 1996;6(9):1473–8.
[46] Tung CYM, Dynes PJ. J Appl Polym Sci 1982;27:569–74.
[47] Calabrese L, Valenza A. Eur Polym J 2003;39(7):1355–63.
[48] Smith BC. Quantitative spectroscopy: theory and practice. San Diego: Academic Press; 2002, p. 64–67.
[49] Lee JY, Shim MJ, Lee HK, Kim SW. J Appl Polym Sci 2001;82: 2372–80.
[50] Pasch H, Unvericht R, Resch M. Angew Makromol Chem 1993;212: 191–200.
[51] Pretsch E, Clerc T, Seibl J, Simon W. Tabellen zur Strukturaufklärung Organischer Verbindungen mit Spektroscopischen Metoden. Berlin: Springer; 1976.
[52] Berti G, Bottari F. J Org Chem 1960;25:1286–92.
[53] Ronda JC, Serra A, Cadiz V. Macromol Chem Phys 1999;200: 221–30.
[54] Blumstein A, Thomas O. Macromolecules 1982;15:1264–7.
[55] Blumstein A, Maret G, Vilasagar S. Macromolecules 1981;14: 1543–5.
[56] Yandrasits MA, Cheng SZD, Zhang A, Cheng J, Wunderlich B, Percec V. Macromolecules 1992;25:2112–21.
[57] Gray GW. Molecular structure and the properties of liquid crystals. London: Academic Press; 1972.
[58] Ortiz C, Ober CK, Kramer EJ. Polymer 1998;39(16):3713–8.
[59] De Vries A. Mol Cryst Liq Cryst 1985;131:125–45.